

STRUCTURE NOTE

Structure of the OSR1 kinase, a hypertension drug target

Fabrizio Villa,^{1,2} Maria Deak,² Dario R. Alessi,² and Daan M. F. van Aalten^{1*}

¹ Division of Biological Chemistry and Drug Discovery, School of Life Sciences, University of Dundee, Dundee DD1 5EH, Scotland

² MRC Protein Phosphorylation Unit, MSI/WTB complex, University of Dundee, Dow Street, Dundee DD1 5EH, Scotland

Key words: Gordon's syndrome; hypertension; protein kinase; protein structure.

INTRODUCTION

The oxidative stress-responsive kinase-1 (OSR1) and STE20/SPS1-related proline/alanine-rich kinase (SPAK) interact, phosphorylate, and stimulate the activity of the cation-chloride cotransporters (NKCC1, NKCC2, and the Na⁺:Cl⁻ cotransporter (NCC)).^{1–4} These cotransporters play key roles in regulating salt intake and secretion from cells (reviewed in Refs. 5,6). Some of the most commonly prescribed blood pressure-lowering thiazide drugs exert their physiological effects by inhibiting NCC. The SPAK and OSR1 enzymes are phosphorylated and activated by the WNK1 and WNK4 protein kinases in response to hyperosmotic and hypotonic stress.^{7–9} This may increase blood pressure by stimulating phosphorylation and activation of NCC.³ Consistent with this, WNK1 and WNK4 genes are mutated in patients suffering from an inherited hypertension and hyperkalemia (elevated plasma K⁺) disorder, termed pseudohypoaldosteronism type II.^{10,11}

SPAK and OSR1 are 68% identical in sequence and possess a highly similar kinase catalytic domain as well as a conserved C-terminal (CCT) domain.⁴ The CCT domain operates as a docking site enabling OSR1 and SPAK to interact with RFXV (Arg-Phe-Xaa-Val) motifs found in both their upstream activators as well as their substrates.^{2,12,13} Structural analysis revealed that the CCT domain forms a novel protein fold.¹⁴ The WNK1 and WNK4 protein kinases phosphorylate OSR1 and SPAK at their T-loop residue within the kinase catalytic domain (Thr185 in OSR1, Thr233 in SPAK).⁹

It is possible that inhibition of the WNK/OSR1/NCC phosphorylation cascade with kinase inhibitors may pro-

vide an alternative chemotherapeutic approach to direct inhibition of NCC. As a first step towards this, we describe the first crystal structure of an OSR1 fragment encompassing the catalytic domain of the enzyme.

METHODS

General methods and DNA constructs

Restriction enzyme digests, DNA ligations, and other recombinant DNA procedures were performed using standard protocols. The cloning of human OSR1 has been described previously.⁹

Cloning, Expression, and crystallization of the OSR1 kinase domain

A fragment corresponding to residues 1–303 of OSR1 (NCBI accession number O95747) was cloned into pGEX-6P-1 (GE Healthcare) as a *Bam*HI-*Not*I insert. BL21 *E. coli* cells were transformed with the pGEX-OSR1(1–303) and were grown at 37°C until the OD₆₀₀ reached 0.8. Subsequently, 0.15 mM IPTG was added,

Fabrizio Villa's current address is Department of Experimental Oncology, European Institute of Oncology, Via Adamello 16, 20139 Milan, Italy
Grant sponsors: Wellcome Trust Senior Research Fellowship, Lister Research Prize, Association for International Cancer Research, Diabetes UK, The Medical Research Council, the Moffat Charitable Trust.

*Correspondence to: Daan M. F. van Aalten, Division of Biological Chemistry and Drug Discovery, School of Life Sciences, University of Dundee, Dundee DD1 5EH, Scotland. E-mail: dava@davapc1.bioch.dundee.ac.uk

Received 19 May 2008; Revised 1 July 2008; Accepted 14 July 2008
Published online 2 September 2008 in Wiley InterScience (www.interscience.wiley.com). DOI: 10.1002/prot.22238

and the culture was grown at 26°C for 18 h. GST-OSR1 recombinant protein was affinity purified following standard protocol and the affinity tag removed through incubation with PreScission protease. OSR1 was then further purified on a Superdex 200 26/60 (GE Healthcare) equilibrated against 25 mM Tris/HCl pH 7.5, 150 mM NaCl and 1 mM DTT. Pure OSR1(1-303) protein was concentrated to 17 mg/ml and five-fold molar excess of a nonhydrolyzable ATP analogue (AMP-PNP) was added. Vapor diffusion crystallization experiments were set up by mixing 0.75 μ L of protein, 0.75 μ L of mother liquor (0.15M magnesium chloride, 0.1M Tris pH 8, and 20% PEG3350).

X-ray data collection, structure solution and refinement

The crystals were cryoprotected in a solution containing mother liquor and 15% v/v PEG400, and then frozen in a nitrogen cryostream. Crystals used for phasing were soaked in mother liquor containing 10mM AuCN for \sim 18 h and cryoprotected as earlier. A two-wavelength MAD data set was collected from the AuCN-soaked crystals (Table I). Phases were calculated with SOLVE,¹⁵ finding 11 Au sites with a figure of merit of 0.44. With the help of FFFear¹⁶ and MOLREP,¹⁷ four OSR1 molecules were located and the noncrystallographic symmetry operators found. Solvent flattening and four-fold averaging were then performed with DM¹⁸ and the resulting map was used as input for warpNtrace.¹⁹ Iterative model building with COOT²⁰ and refinement with REFMAC²¹ in which the four molecules in the asymmetric unit were refined initially with strict NCS, but in the final stages independently, yielding the final model with statistics shown in Table I. Atomic coordinates and structure factors have been deposited in the Protein Data Bank under the PDB code 2vwi.

SAXS sample preparation, data collection and analysis

Full length OSR1(1-527) was expressed and purified as described earlier, concentrated to 8.6 mg/mL and 10mM DTT was added immediately prior to synchrotron measurements. Scattering data were collected at the beamline 2.1, Daresbury (UK). Data were corrected for buffer scattering and checked for radiation damage using the XOTOKO²² software. The scattering intensities curves were then analyzed with GNOM²³ and the D_{\max} and radius of gyration (R_g) were calculated.

Homology modeling

Homology modeling for OSR1 kinase active conformation was performed using the MODELLER software.²⁴ All figures were made with PyMOL.

Table I
Crystallographic Data and Refinement Statistics

	OSR1-Peak	OSR1-Inflexion
Beamline	BM14	BM14
	λ_1	λ_2
Wavelength (Å)	1.033	1.039
Space Group	P2 ₁ 2 ₁ 2 ₁	P2 ₁ 2 ₁ 2 ₁
Unit Cell (Å)	$a = 74.13$ $b = 99.90$ $c = 158.52$	$a = 74.20$ $b = 100.11$ $c = 158.78$
Resolution (Å)	20.0–2.15 (2.23–2.15)	20.0–2.40 (2.49–2.40)
Observed reflections	3,400,729	2,127,894
Unique reflections	65,284	47,079
Redundancy	13.6 (3.9)	9.2 (4.9)
Completeness (%)	98.7 (88.2)	99.8 (98.1)
R_{merge}^a	0.065 (0.3)	0.055 (0.242)
$I / \sigma I$	48.6 (2.8)	43.9 (5.1)
R_{cryst}^b	0.252	
R_{free}^c	0.286	
$\langle B_{\text{protein}} \rangle$ (Å ²)	41.4	
Number of groups		
Protein residues	1072	
Water	295	
Ligand atoms	134	
Mg ²⁺ atoms	4	
RMSD from ideal geometry		
Bond length (Å)	0.006	
Bond angles (°)	0.964	
Ramachandran plot (%)		
Most favoured region	90.7	
Additionally allowed	8.0	
Generously allowed	1.3	

Values in parenthesis are reflections from the highest resolution shell. All data were included in the refinement.rmsd, root mean squares deviation.

^a $R_{\text{merge}} = \sum |I - \langle I \rangle| / \sum I$, where, I is the observed intensity of a reflection and $\langle I \rangle$ is the average intensity obtained from multiple observations of symmetry-related reflections.

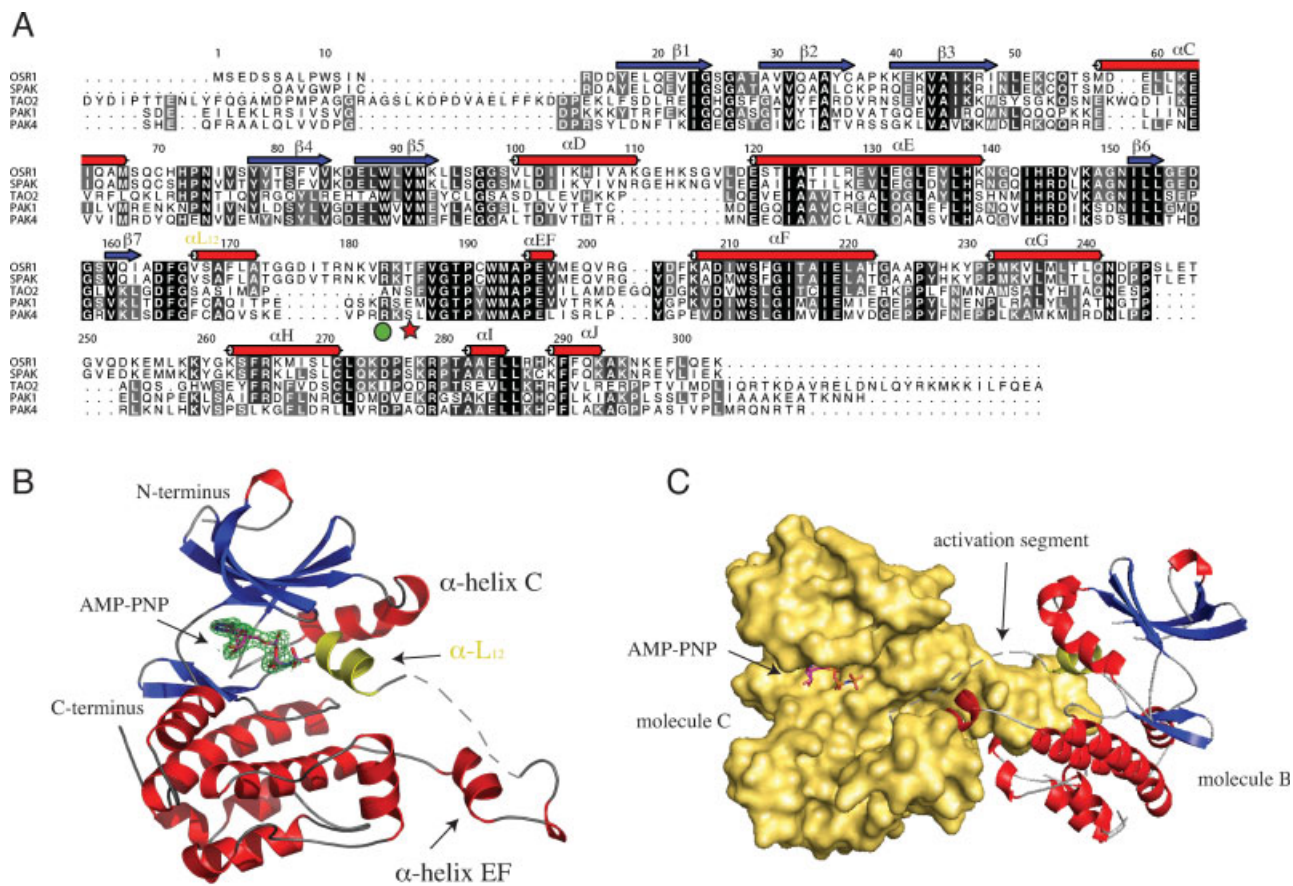
^b $R_{\text{cryst}} = \sum ||F_o| - |F_c|| / \sum |F_o|$, where F_o and F_c are the observed and calculated structure factor amplitudes respectively.

^c R_{free} is equivalent to R_{cryst} for a 5% subset of reflections not used in the refinement.

RESULTS AND DISCUSSION

Structure of the OSR1 kinase domain

Limited trypsin proteolysis of full-length protein led to the identification of a stable proteolytic fragment encompassing the catalytic domain [Fig. 1(A)]. OSR1(1-303) was cloned, expressed in *E. coli* and the protein crystallized from PEG solutions in presence of an excess of AMP-PNP. The OSR1 kinase domain assumes the classical bilobal kinase fold [Fig. 1(B)], which is similar to the canonical kinase structure of cyclic AMP-dependent protein kinase (PKA).²⁵ The structure consists of a 5-stranded anti-parallel β -sheet with an α -helix (α C) connecting strands β 3– β 4 whilst the C-terminal lobe is mainly α -helical [Fig. 1(B)]. The overall structure of the OSR1 kinase domain is similar to the recently determined structures of some STE kinase group members (rms deviations for all C α atoms in the TAO2,²⁶ PAK1,²⁷ PAK4,²⁸ and MEK1²⁹ kinase domains are 1.3, 1.5, 1.2, and 1.5 Å, respectively).

**Figure 1**

Overall structure of the OSR1 kinase domain. (A) Multiple sequence alignment of human OSR1 and SPAK kinases and some members of the STE group previously crystallized (TAO2, PAK1, and PAK4). Secondary structure elements and numbering are according to human OSR1. TAO2, PAK1, and PAK4 sequences correspond to the protein crystallized and deposited in the PDB database (PDB codes 1U5R, 1YHV, and 2BVA, respectively). The threonine (Thr185) targeted by WNK is labelled with a red star and Arg183 with a green circle. (B) Cartoon representation of the OSR1 kinase domain, colored in blue and red (β -strands and α -helices, respectively) apart for α -helix L_{12} (yellow). The secondary structure elements are labeled in agreement with [Fig. 1(A)]. The AMP-PNP molecule in the OSR1 active site is represented as sticks (magenta) with an unbiased $F_o - F_c$ electron density map (green), (σ level = 2.5). (C) Domain-exchanged kinase dimer. The activation segment from each monomer extends to form an extensive intermolecular interface. Molecular surface (yellow) is shown for one monomer, while the other monomer is shown as a cartoon. The disordered activation segment is represented as dotted lines and bound nucleotide is shown as stick (magenta).

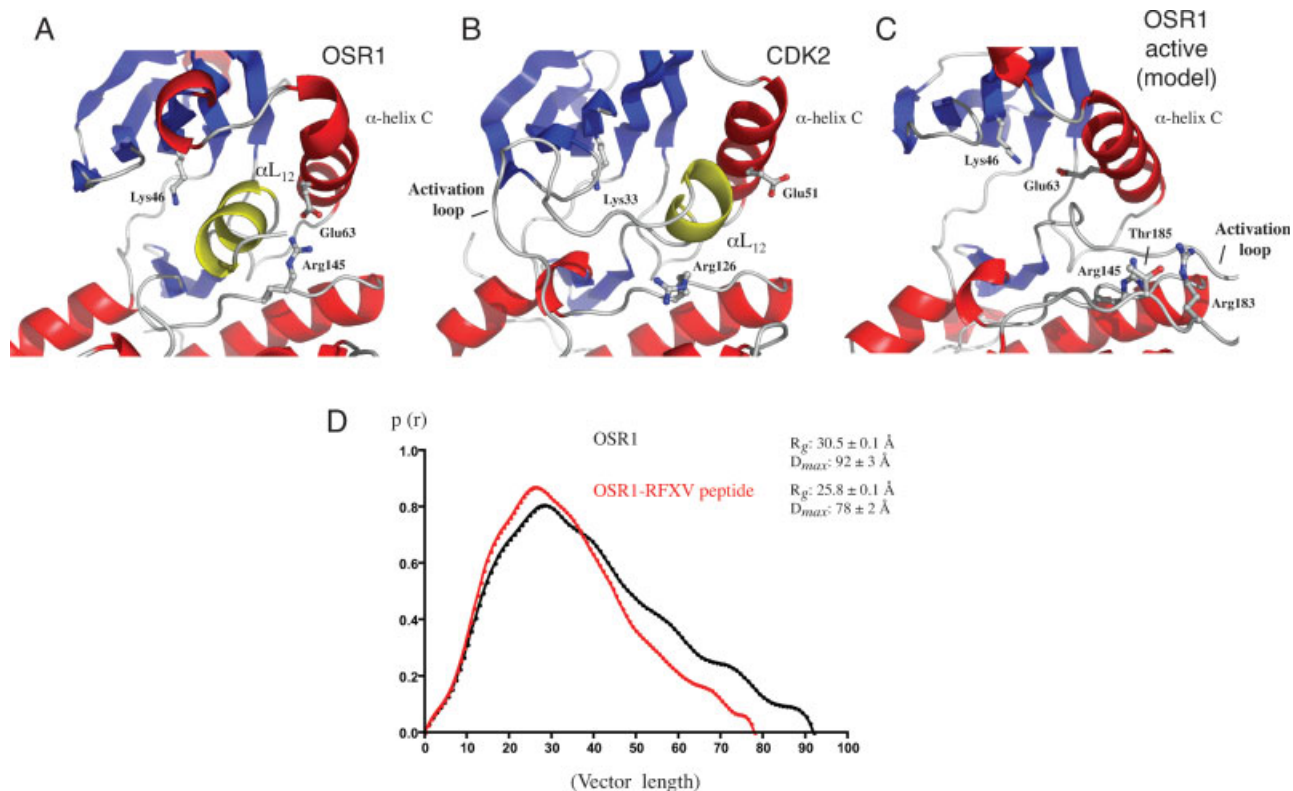
The OSR1 kinase domain in the crystal adopts an inactive conformation, as evidenced by the absence of electron density for the activation segment (residues 175 to 189) including Thr185, the target of phosphorylation by WNK isoforms.^{7–9} Interestingly, the active site of the kinase is partially occupied by the N-terminus of the activation segment assuming an unusual two-turn helix, topologically resembling helix αL_{12} of CDK2³⁰ [Figs. 1(A) and 2(A–B)]. The conserved catalytic ion pair between Lys46 from β -strand 2 and Glu63 from α -helix C is also disrupted by steric hindrance of αL_{12} (positioning Lys46 and Glu63 12.5 Å apart) [Fig. 2(A)].

Activation segment dimerization

The most striking feature of the OSR1 structure is an exchange of activation segments between symmetry-

related molecules. The four independent OSR1 molecules are arranged as pairs of dimers [Fig. 1(C)] and superposition of the α -carbon traces of the four molecules reveals a high degree of similarity with an average rmsd of 0.65 Å. This contact mainly involves hydrophobic interactions between the two molecules. Several residues, such as Trp192, Met193, Leu197, and Met198 from helix αEF are occupying a hydrophobic pocket made up from residues Met233, Val235, Leu236, and Leu240 (helix αG), residues Trp211 and Ile215 (helix αF) of the neighboring molecule [Fig. 1(C)].

Activation segment exchange between kinases has recently been highlighted as a mechanism of trans-auto-phosphorylation in kinases such as CHK2,³¹ SLK, LOK, and DAPK3.³² Although OSR1 is phosphorylated at its activation segment *in vivo* by the WNK enzymes,^{7–9} it is

**Figure 2**

OSR1 active conformation and conformational change induced by RFXV peptide binding. (A) OSR1 activation segment with the secondary structure elements and the residues discussed in the text represented as cartoon and sticks, respectively, colored in blue and red (β -strands and α -helices). Shown in sticks are Lys46, Glu63, and Arg145. (B) CDK2 activation segment with the secondary structure elements and the residues discussed in the text represented as cartoon and sticks, respectively, colored in blue and red (β -strands and α -helices). Shown in sticks are Lys33, Glu51, and Arg126. (C) Model of the active conformation of the OSR1 kinase domain with the activation segment and α -helix C represented as cartoon. Shown in sticks are Lys46, Glu63, Arg145, Arg183, and Thr185. (D) Distance-distribution function are for the OSR1(1-527) protein and for OSR1(1-527)-RFXV peptide complex as determined by SAXS. Radius of gyration and D_{max} are also indicated. Vector length is shown as Å and $p(r)$ as arbitrary unit.

not clear whether the (homo)-dimerization seen in the crystal structure is structurally reminiscent of the trans-phosphorylation event or simply a crystallographic artefact. A recent study has shown that a fragment encompassing the catalytic kinase domain of OSR1(1-344) oligomerises *in vivo* in a similar manner as other STE group members.⁷ However, the OSR1(1-303) kinase domain is monomeric in solution as judged by size exclusion chromatography (data not shown) and from the X-ray solution scattering calculated parameters [Fig. 2(D)].

OSR1/SPAK active conformation

In an attempt to understand the molecular mechanism by which OSR1 is activated by WNK isoforms, we crystallized the Thr185Glu mutant, in order to mimic a form of OSR1 that was phosphorylated. However inspection of the electron density revealed that the OSR1[T185E] mutant was not in an active conformation, and we therefore decided to generate a homology-based structural model of OSR1 active conformation based on a multiple

sequence alignment and the known structures of the STE20 related kinases [Fig. 1(A)]. The homology model of the OSR1 active conformation suggests that mainly Arg183, and Arg145 (RD motif) would be candidates for stabilizing the phospho-Thr185 [Figs. 1(A) and 2(C)], resembling the activation mechanism observed in the PAK subfamily members.^{27,28} A multiple sequence alignment of OSR1, the closely related SPAK and other STE group members already crystallized (TAO2, PAK1, and PAK4), reveals that these residues are conserved in OSR1/SPAK [Fig. 1(A)]. Thus, this suggests that the active conformation of OSR1 and SPAK may be achieved through a similar mechanism previously observed for the PAK subfamily members PAK1,²⁷ PAK4²⁸ [Figs. 1(A) and 2(C)] and reminiscent of PhK.³³

Binding of OSR1 to the RFXV motif induces a large conformational change

Full length OSR1 in presence or absence of RFXV motif-containing peptides has so far resisted crystalliza-

tion. We therefore attempted to study the solution conformation of full length OSR1 by small angle X-ray scattering (SAXS). For these studies, full-length OSR1(1-527) over-expressed and purified from *E. coli* was subjected to SAXS measurements in absence and in presence of a peptide derived from human WNK4, encompassing the RFXV motif necessary for binding to the OSR1 CCT domain.^{14,34} From the resulting scattering curves, the radii of gyration (R_g) and maximum diameters (D_{max}) were calculated [Fig. 2(D)]. OSR1 in the absence of the RFXV peptide assumed an elongated shape with a radius of gyration of $30.5 \pm 0.1 \text{ \AA}$ and a D_{max} of $92 \pm 3 \text{ \AA}$ [Fig. 2(D)]. Addition of the WNK4 peptide to the OSR1 solution resulted in a markedly more compact molecule with a radius of gyration of $25.8 \pm 0.1 \text{ \AA}$ and a D_{max} of $78 \pm 2 \text{ \AA}$, suggesting that peptide binding induces a significant conformational change [Fig. 2(D)]. The reduction of D_{max} and R_g of the OSR1-RFXV peptide complex in solution might suggest a large movement of the conserved C-terminal (CCT) domain towards the catalytic domain of the protein [Fig. 2(D)]. It is therefore possible that the binding of the conserved C-terminal (CCT) to the RFXV peptide induces a conformational change required for OSR1 to be efficiently phosphorylated by WNKs and to efficiently phosphorylate the substrates without affecting the catalytic efficiency of the enzyme.

ACKNOWLEDGMENTS

The authors thank the European Synchrotron Radiation Facility (Grenoble, France) for beam time at BM14 and the Synchrotron Radiation Source (Daresbury, UK) for beam time at the 2.1 station.

REFERENCES

- Dowd BF, Forbush B. PASK (proline-alanine-rich STE20-related kinase), a regulatory kinase of the Na-K-Cl cotransporter (NKCC1). *J Biol Chem* 2003;278:27347–27353.
- Piechotta K, Garbarini N, England R, Delpire E. Characterization of the interaction of the stress kinase SPAK with the Na⁺-K⁺-2Cl⁻ cotransporter in the nervous system: evidence for a scaffolding role of the kinase. *J Biol Chem* 2003;278:52848–52856.
- Richardson C, Rafiqi FH, Karlsson HK, Moleleki N, Vandewalle A, Campbell DG, Morrice NA, Alessi DR. Activation of the thiazide-sensitive Na⁺-Cl⁻ cotransporter by the WNK-regulated kinases SPAK and OSR1. *J Cell Sci* 2008;121(Part 5):675–684.
- Delpire E, Gagnon KB. SPAK and OSR1: STE20 kinases involved in the regulation of ion homeostasis and volume control in mammalian cells. *Biochem J* 2008;409:321–331.
- Flatman PW. Cotransporters WNKs and hypertension: important leads from the study of monogenic disorders of blood pressure regulation. *Clin Sci (Lond)* 2007;112:203–216.
- Gamba G. Role of WNK kinases in regulating tubular salt and potassium transport and in the development of hypertension. *Am J Physiol Renal Physiol* 2005;28:245–252.
- Anselmo AN, Earnest S, Chen W, Juang YC, Kim SC, Zhao Y, Cobb MH. WNK1 and OSR1 regulate the Na⁺, K⁺, 2Cl⁻ cotransporter in HeLa cells. *Proc Natl Acad Sci USA* 2006;103:10883–10888.
- Moriguchi T, Urushiyama S, Hisamoto N, Iemura S, Uchida S, Natsume T, Matsumoto K, Shibuya H. WNK1 regulates phosphorylation of cation-chloride-coupled cotransporters via the STE20-related kinases SPAK and OSR1. *J Biol Chem* 2005;280:42685–42693.
- Vitari AC, Deak M, Morrice NA, Alessi DR. The WNK1 and WNK4 protein kinases that are mutated in Gordon's hypertension syndrome phosphorylate and activate SPAK and OSR1 protein kinases. *Biochem J* 2005;391(Part 1):17–24.
- Kahle KT, Rinehart J, Giebisch G, Gamba G, Hebert SC, Lifton RP. A novel protein kinase signaling pathway essential for blood pressure regulation in humans. *Trends Endocrinol Metab* 2008;19:91–95.
- Wilson FH, Disse-Nicodeme S, Choate KA, Ishikawa K, Nelson-Williams C, Desitter I, Gunel M, Milford DV, Lipkin GW, Achard JM, Feely MP, Dussol B, Berland Y, Unwin RJ, Mayan H, Simon DB, Farfel Z, Jeunemaitre X, Lifton RP. Human hypertension caused by mutations in WNK kinases. *Science* 2001;293:1107–1112.
- Piechotta K, Lu J, Delpire E. Cation chloride cotransporters interact with the stress-related kinases Ste20-related proline-alanine-rich kinase (SPAK) and oxidative stress response 1 (OSR1). *J Biol Chem* 2002;277:50812–50819.
- Gagnon KB, England R, Delpire E. Characterization of SPAK and OSR1, regulatory kinases of the Na-K-2Cl cotransporter. *Mol Cell Biol* 2006;26:689–698.
- Villa F, Goebel J, Rafiqi FH, Deak M, Thastrup J, Alessi DR and van Aalten DMF. Structural insight into the recognition of substrates and activators by the OSR1 kinase. *EMBO Rep* 2007;8:839–845.
- Terwillinger TC, Berendzen J. Automated MAD and MIR structure solution. *Acta Crystallogr D* 1999;55:849–861.
- Collaborative Computational Project N. The CCP4 suite: programs for protein crystallography. *Acta Crystallogr D Biol Crystallogr* 1994;50:760–763.
- Vagin A, Teplyakov A. MOLREP: an automated program for molecular replacement. *J Appl Crystallogr* 1997;30:1022–1025.
- Cowan K, Main P. Miscellaneous algorithms for density modification. *Acta Crystallogr D Biol Crystallogr* 1998;54(Part 4):487–493.
- Perrakis A, Morris R, Lamzin VS. Automated protein model building combined with iterative structure refinement. *Nat Struct Biol* 1999;6:458–463.
- Emsley P, Cowtan K. Coot: model-building tools for molecular graphics. *Acta Crystallogr D Biol Crystallogr* 2004;60(Part 12 Part 1): 2126–2132.
- Murshudov GN, Vagin AA, Dodson EJ. Refinement of macromolecular structures by the maximum-likelihood method. *Acta Crystallogr D Biol Crystallogr* 1997;53(Part 3):240–255.
- Boulin C, Kempf R, Koch MHJ, McLaughlin SM. Data appraisal, evaluation and display for synchrotron radiation experiments: hardware and software. *Nucl Instrum Methods* 1986;A249:399–407.
- Semenyuk AV, Svergun DI. Gnom—a Program Package for Small-Angle Scattering Data-Processing. *J Appl Crystallogr* 1991;24:537–540.
- Sali A, Blundell TL. Comparative Protein Modeling by Satisfaction of Spatial Restraints. *J Mol Biol* 1993;234:779–815.
- Knighton DR, Zheng JH, Ten Eyck LF, Ashford VA, Xuong NH, Taylor SS, Sowadski JM. Crystal structure of the catalytic subunit of cyclic adenosine monophosphate-dependent protein kinase. *Science* 1991;253:407–414.
- Zhou T, Raman M, Gao Y, Earnest S, Chen Z, Machius M, Cobb MH, Goldsmith EJ. Crystal structure of the TAO2 kinase domain: activation and specificity of a Ste20p MAP3K. *Structure* 2004;12: 1891–1900.
- Lei M, Robinson MA, Harrison SC. The active conformation of the PAK1 kinase domain. *Structure* 2005;13:769–778.
- Eswaran JLW, Debreczeni JE, Filippakopoulos P, Turnbull A, Fedorov O, Deacon SW, Peterson JR, Knapp S. Crystal structures of

- the p21-activated kinases PAK4, PAK5 and PAK6 reveal catalytic domain plasticity of active group II PAKs. *Structure* 2007;15:201–213.
29. Ohren JF, Chen H, Pavlovsky A, Whitehead C, Zhang E, Kuffa P, Yan C, McConnell P, Spessard C, Banotai C, Mueller WT, Delaney A, Omer C, Sebolt-Leopold J, Dudley DT, Leung IK, Flamme C, Warmus J, Kaufman M, Barrett S, Teclé H, Hasemann CA. Structures of human MAP kinase kinase 1 (MEK1) and MEK2 describe novel noncompetitive kinase inhibition. *Nat Struct Mol Biol* 2004;11:1192–1197.
 30. De Bondt HL, Rosenblatt J, Jancarik J, Jones HD, Morgan DO, Kim SH. Crystal structure of cyclin-dependent kinase 2. *Nature* 1993;363:595–602.
 31. Oliver AW, Paul A, Boxall KJ, Barrie SE, Aherne GW, Garrett MD, Mitnacht S, Pearl LH. Trans-activation of the DNA-damage signalling protein kinase Chk2 by T-loop exchange. *Embo J* 2006;25:3179–3190.
 32. Pike AC, Rellos P, Niesen FH, Turnbull A, Oliver AW, Parker SA, Turk BE, Pearl LH, Knapp S. Activation segment dimerization: a mechanism for kinase autophosphorylation of non-consensus sites. *Embo J* 2008;27:704–714.
 33. Owen DJ, Noble ME, Garman EF, Papageorgiou AC, Johnson LN. Two structures of the catalytic domain of phosphorylase kinase: an active protein kinase complexed with substrate analogue and product. *Structure* 1995;3:467–482.
 34. Vitari AC, Thastrup J, Rafiqi FH, Deak M, Morrice NA, Karlsson HK, Alessi DR. Functional interactions of the SPAK/OSR1 kinases with their upstream activator WNK1 and downstream substrate NKCC1. *Biochem J* 2006;397:223–231.